Chapter 4:

Results and Discussion 1

Cloning, Expression and Purification of Recombinant full-length huntingtin proteins with SA or SD mutations

Phosphorylation of many proteins, at serine (S), threonine (T) or tyrosine (Y) residues, regulates their functional activities, turnover [1] and nuclear transport [2]. Several phosphorylation sites have been predicted in huntingtin and some sites have been confirmed; Thr3 and Ser13 and Ser16 [3,4], as well as Ser421, which is phosphorylated by AKT [5]. Some of these sites have been implicated in toxicity of mutant huntingtin while others are demonstrated to be of protective nature. Some of the most compelling evidence for the protective nature of huntingtin phosphorylation comes from analysis of full-length human huntingtin Ser13 and Ser16 phosphorylation in BAC transgenic mice [6]. Expression of phosphomimetic huntingtin, wherein serine was changed to aspartate (SD) or, alternatively, expression of phosphor-resistant huntingtin wherein serine is changed to alanine (SA), demonstrated that while, both SA and SD mutant huntingtin proteins retained essential huntingtin function in rescuing Hdh knockout mouse phenotypes, only the SD mutant protein was associated with a striking absence of the motor, psychiatric and neuropathological phenotypes and notable decrease in mutant huntingtin aggregates [6]. This result strongly suggest that huntingtin phosphorylation at Ser13/Ser16 can directly or indirectly prevent the toxic consequences associated with expanded polyQ huntingtin. However, the mechanism behind this reversal of mutant huntingtin toxicity is not very clear and needs further examination. Thus, in this study, we investigate the mechanism of by which mutant huntingtin phosphorylation abrogates its toxicity and propose that it is, at least in part, mediated by its altered interaction with PRC2 complex. Finally, we aim to develop huntingtin phosphorylation as a therapeutic target in HD.

4.1 Characterization of Full-Length Huntingtin Baculovirus Constructs with Ser13 and Ser16 Substituted to Alanine or Aspartate

The pFastBac vectors containing the *HTT* gene with 23, 46, and 78 CAG repeats (HttQ23, HttQ46, and HttQ78) were isolated using the Plasmid Miniprep Kit (QIAGEN). The isolated plasmids were then subjected to electrophoresis on a 0.8% agarose gel, as illustrated in **Fig. 4.1.1**. Following successful isolation, the presence of the target gene within the plasmids was verified via PCR using gene specific primers flanking the CAG repeats resulting in product size according to CAG repeat length, the results of which are depicted in **Fig. 4.1.2**.

Subsequently, these plasmids were transformed into competent *E. coli* DH10Bac cells. The transformed cells were then plated on Luria agar (LA) plates supplemented with kanamycin,

gentamycin, tetracycline, X-gal, and IPTG. These plates were incubated in the dark at 37°C for 24-48 hours. The identification of bacmids containing the gene of interest was accomplished using blue-white screening. In this method, recombinant bacmids have the *HTT* inserted Tn7 mini attachment site present within the LacZα gene, resulting in white colonies in the presence of X-gal and IPTG, in contrast to wild-type *E. coli* DH10Bac cells containing bacmids with intact LacZα gene, produced blue colonies (**Fig. 4.1.3**).

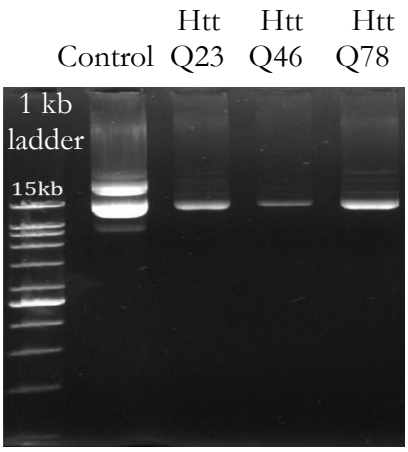

Figure: 4.1.1

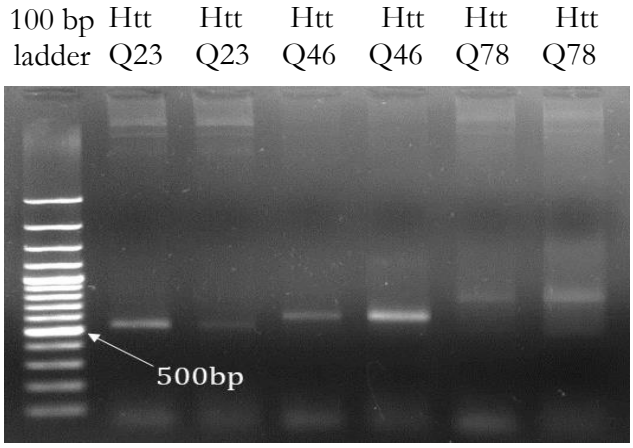

Figure: 4.1.2

Figure 4.1.1: 0.8% Agarose gel showing pFastBac vectors (HttQ23, HttQ46 and HttQ78).

Figure 4.1.2: 1.2% Agarose gel showing PCR confirmation of plasmids.

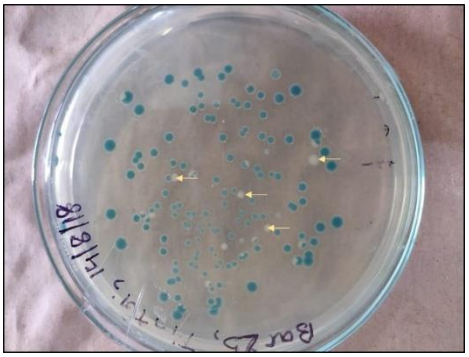

Figure 4.1.3: Blue-white Colonies observed upon transformation of plasmids into *E. coli* DH10Bac.

To confirm the presence of true positive colonies, the white colonies were streaked again onto a medium containing the necessary antibiotics, X-gal, and IPTG. The true white colonies were subsequently inoculated into Luria broth (LB) with the required antibiotics to propagate the bacmids. Bacmids were isolated from these true white colonies using the alkaline lysis method

(**Fig. 4.1.4**). To further verify the presence of the gene of interest in these bacmids, PCR was performed using *HTT* gene-specific primers, as shown in **Fig. 4.1.5**.

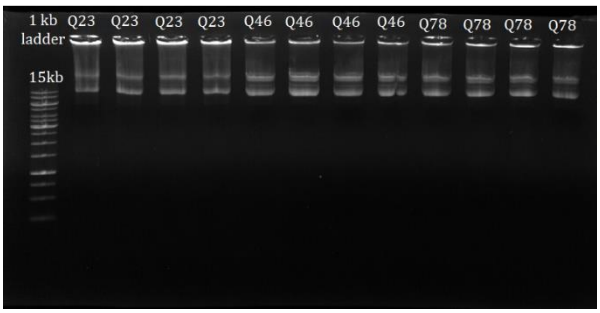

Figure: 4.1.4

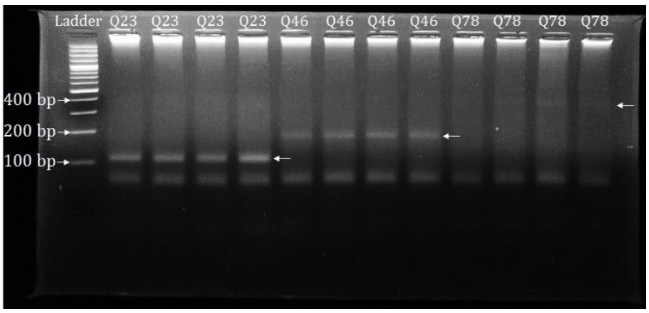

Figure: 4.1.5

Figure 4.1.4: 0.8% Agarose gel showing bacmids (HttQ23, HttQ46 and HttQ78).

Figure 4.1.5: 2% Agarose gel showing PCR verification of HttQ23, HttQ46 and HttQ78 bacmids.

PCR-based site-directed mutagenesis (SDM) was performed to modify serine residues at positions 13 and 16 to alanine and aspartate, respectively. Site-directed mutagenesis is a crucial and widely used tool in molecular biology to generate specific changes in the DNA sequence of a given gene or genome. Following this process, 14 kb PCR products were observed on a 0.8% agarose gel for HttQ23 S13A and HttQ23 S13D, but not for HttQ23 S16A and HttQ23 S16D (**Fig. 4.1.6**). Using gradient PCR, the PCR products for HttQ23 S16D were successfully obtained; however, HttQ23 S16A remained undetected (**Fig. 4.1.7**). As depicted in **Fig. 4.1.8** and **Fig. 4.1.9**, PCR products for HttQ46 S13A, S13D, and S16D were successfully generated, but not for HttQ46 S16A.

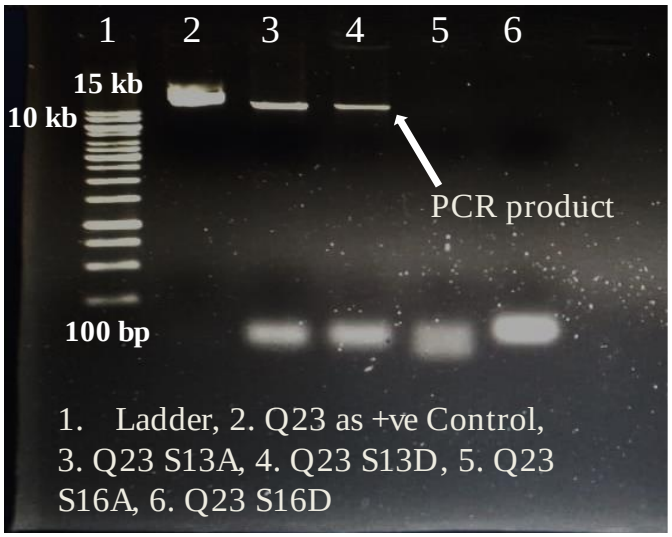

Figure 4.1.6: 0.8% Agarose gel showing site directed mutagenized PCR products for HttQ23.

The obtained PCR products were subsequently subjected to *DpnI* restriction digestion to cleave the template plasmid as *DpnI* cleaves only methylated DNA and mutagenized PCR products are not affected. Following a 2-hour incubation with *DpnI*, a small volume of sample was analyzed on a 0.8% agarose gel to confirm presence of PCR products (**Fig. 4.1.10**). These PCR products were transformed into *E. coli* DH5α competent cells to make them circular. The recombinant plasmids were then isolated using a Plasmid Miniprep Kit and analyzed on a 0.8% agarose gel (**Fig. 4.1.11**). The presence of the gene of interest was verified using PCR with two different sets of primers (**Fig. 4.1.12, 4.1.13, 4.1.14, and 4.1.15**). These plasmids were also sent for sequencing to confirm the mutations.

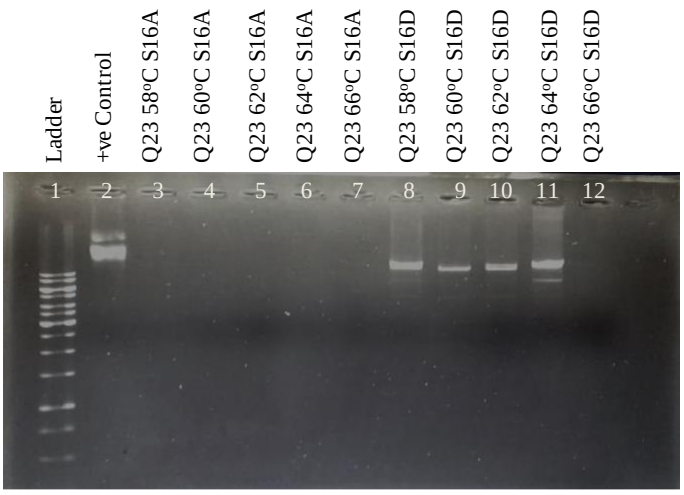

Figure: 4.1.7

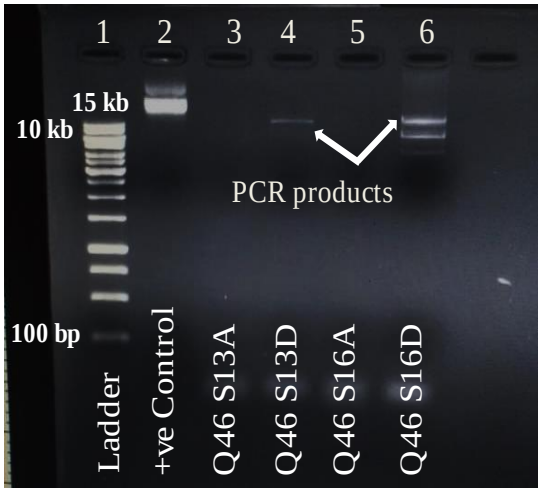

Figure: 4.1.8

Figure 4.1.7: 0.8% Agarose gel showing site directed mutagenized PCR products for HttQ23 as a result of gradient PCR.

Figure 4.1.8: 0.8% Agarose gel showing site directed mutagenized PCR products for HttQ46.

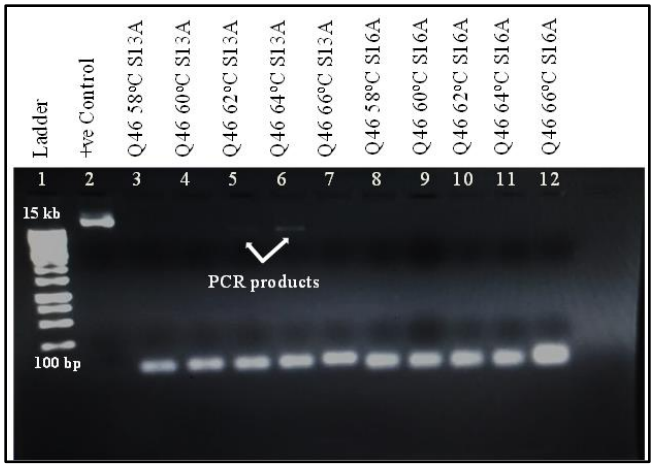

Figure 4.1.9: 0.8% Agarose gel showing site directed mutagenized PCR products for HttQ46 as a result of gradient PCR.

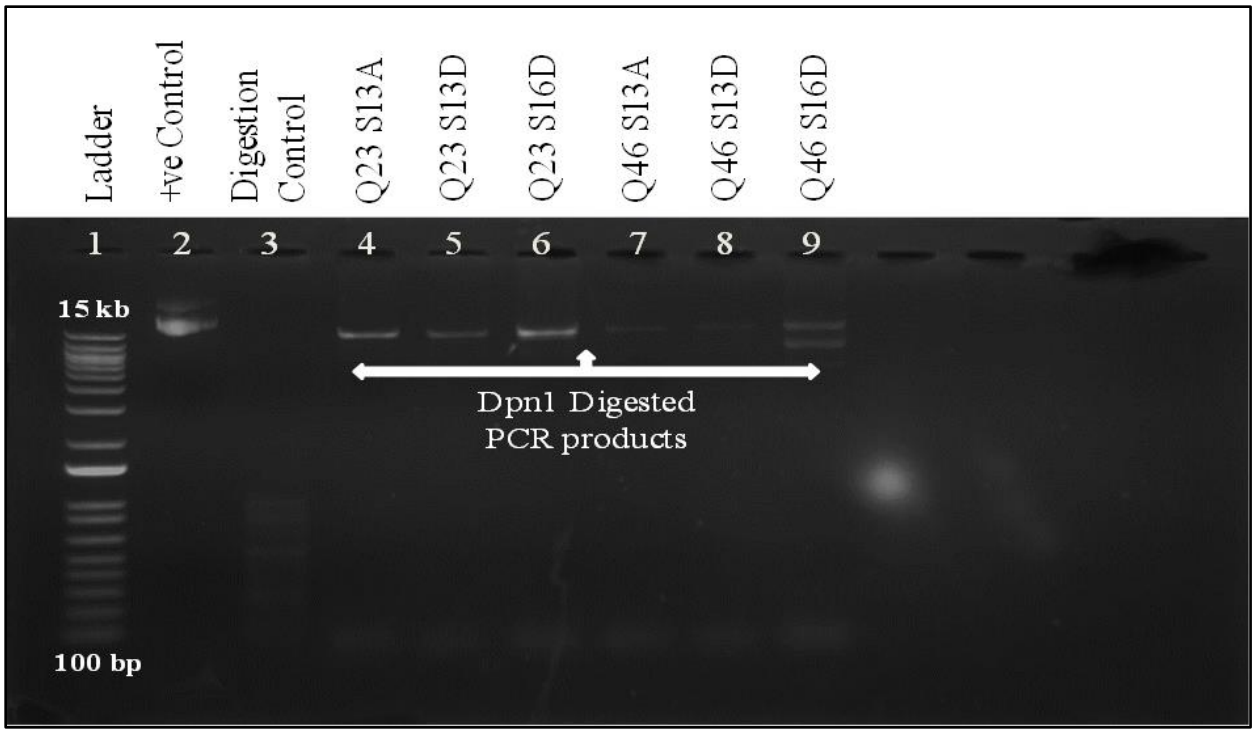

Figure 4.1.10: 0.8% Agarose gel showing *DpnI* digested site directed mutagenized PCR products for HttQ23 and HttQ46.

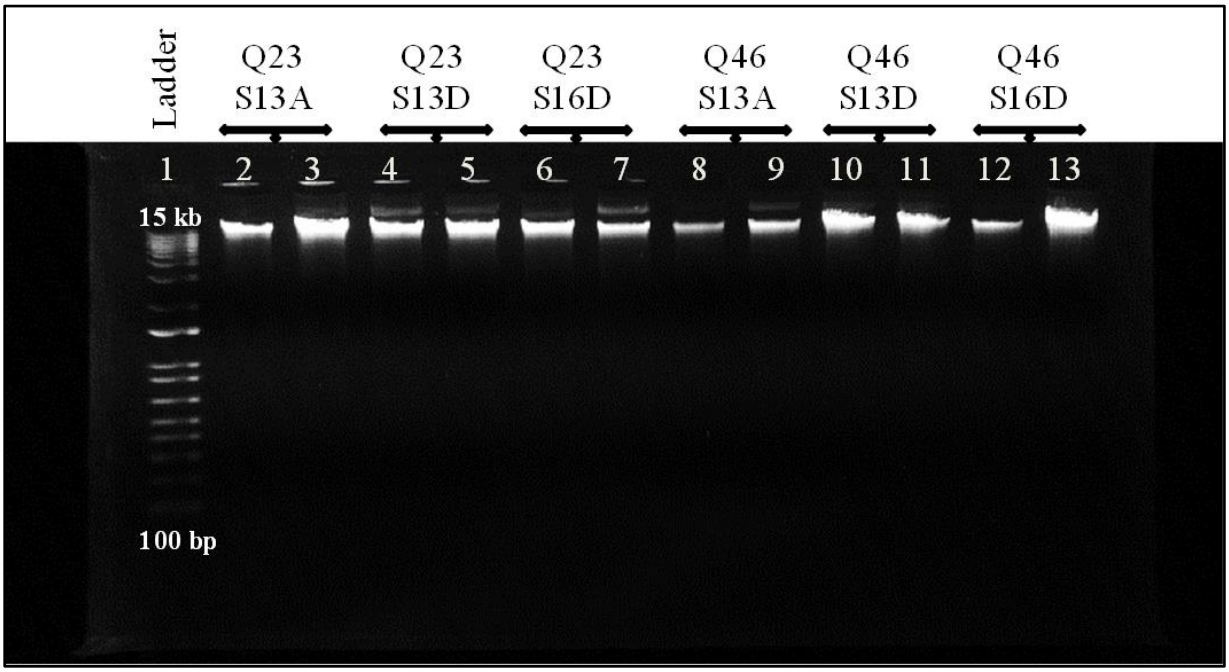

Figure 4.1.11: 0.8% Agarose gel showing recombinant mutagenized plasmids for HttQ23 and HttQ46 isolated using Plasmid Miniprep Kit.

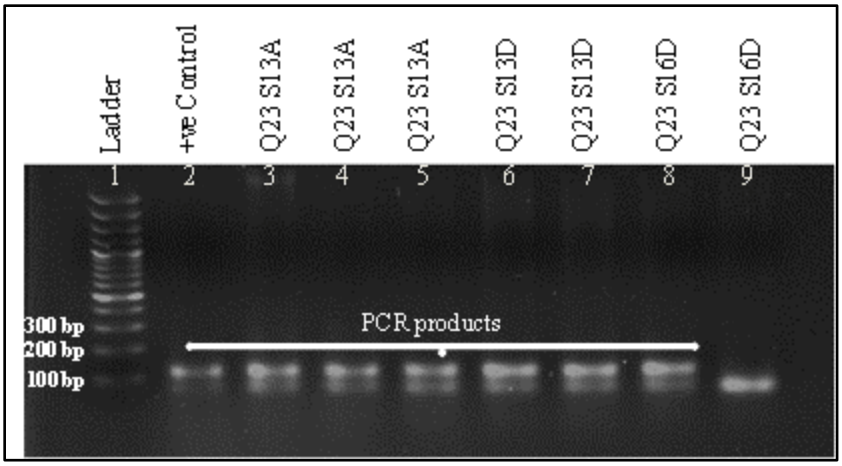

Figure 4.1.12: 2% Agarose gel showing PCR confirmation for HttQ23 recombinant plasmids using HD1 and HD2 primers.

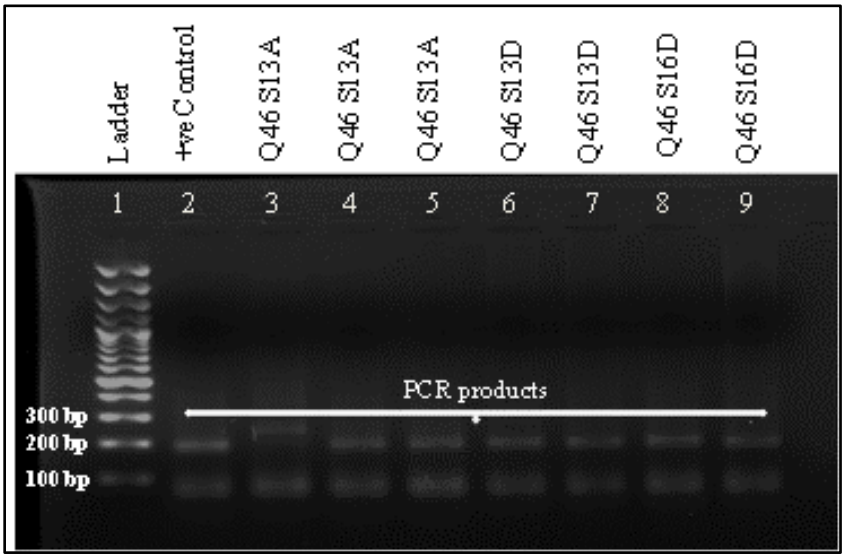

Figure 4.1.13: 2% Agarose gel showing PCR confirmation for HttQ46 recombinant mutagenized plasmids using HD1 and HD2 primers.

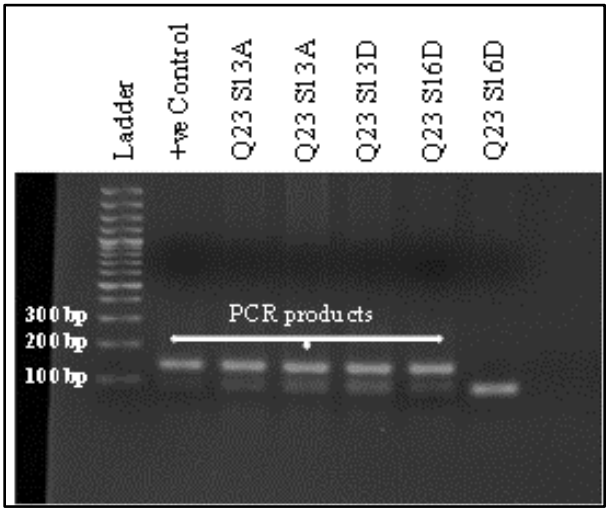

Figure: 4.1.14

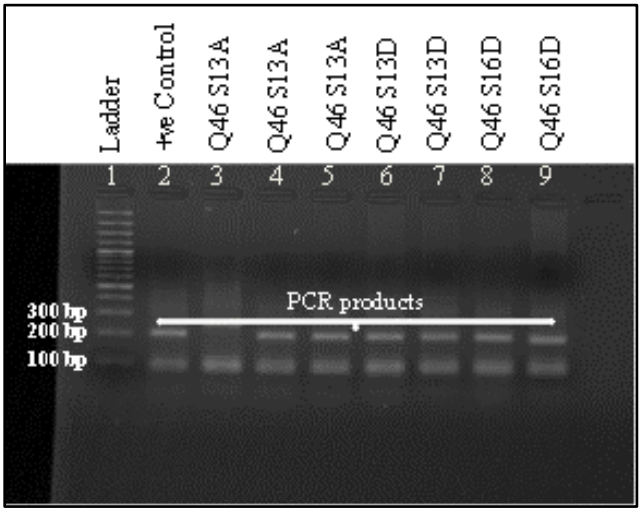

Figure: 4.1.15

Figure 4.1.14: 2% Agarose gel showing PCR confirmation for mutagenized HttQ23 plasmids using Htt SQ primers.

Figure 4.1.15: 2% Agarose gel showing PCR confirmation for mutagenized HttQ46 plasmids using Htt SQ primers.

Subsequently, the plasmids were transformed into competent *E. coli* DH10Bac cells. Bacmids containing the gene of interest were identified using antibiotic selection and blue-white screening (**Fig. 4.1.16 and Fig. 4.1.17**). The bacmids were isolated from true white colonies using the alkaline lysis method, as shown in **Fig. 4.1.18** and **Fig. 4.1.19**. PCR was performed to confirm the presence of the gene of interest in these recombinant bacmids (**Fig. 4.1.20**).

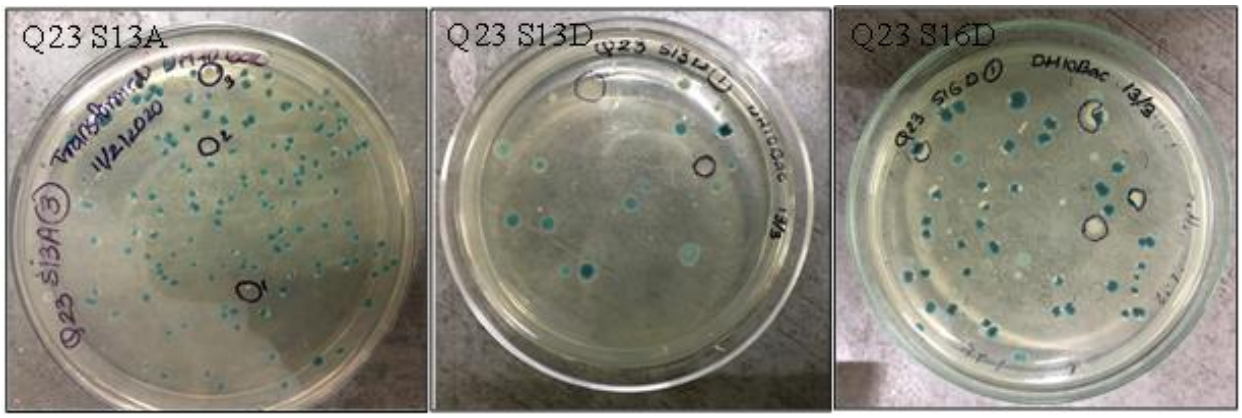

Figure 4.1.16: Blue-white Colonies observed upon transformation of HttQ23 recombinant plasmids into *E. coli* DH10Bac cells.

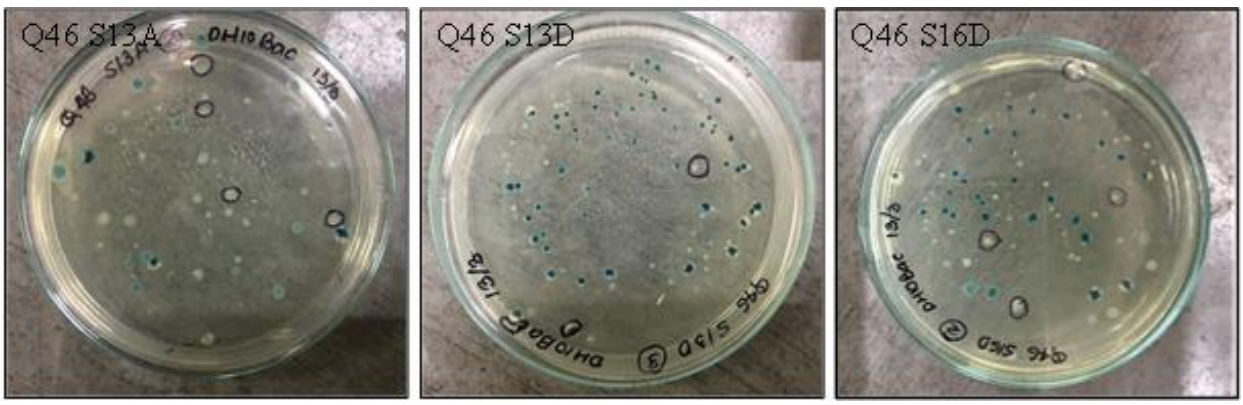

Figure 4.1.17: Blue-white Colonies observed upon transformation of HttQ46 recombinant plasmids into *E. coli* DH10Bac cells.

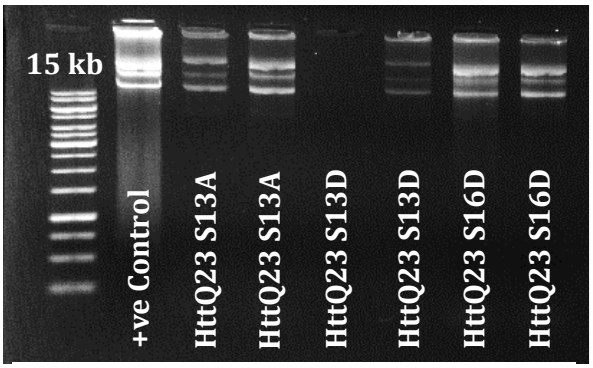

Figure 4.1.18: 0.8% Agarose gel showing HttQ23 S13A, HttQ23 S13D and HttQ23 S16D bacmids.

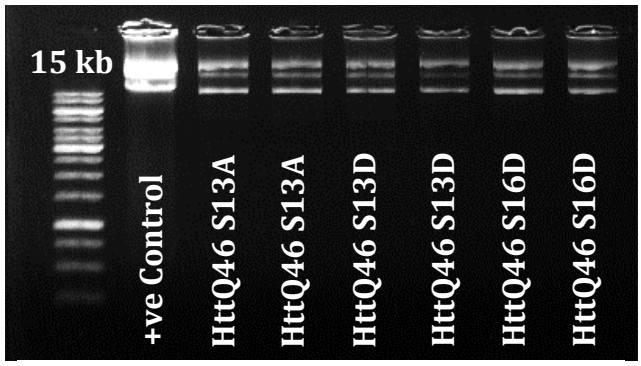

Figure 4.1.19: 0.8% Agarose gel showing HttQ46 S13A, HttQ46 S13D and HttQ46 S16D bacmids.

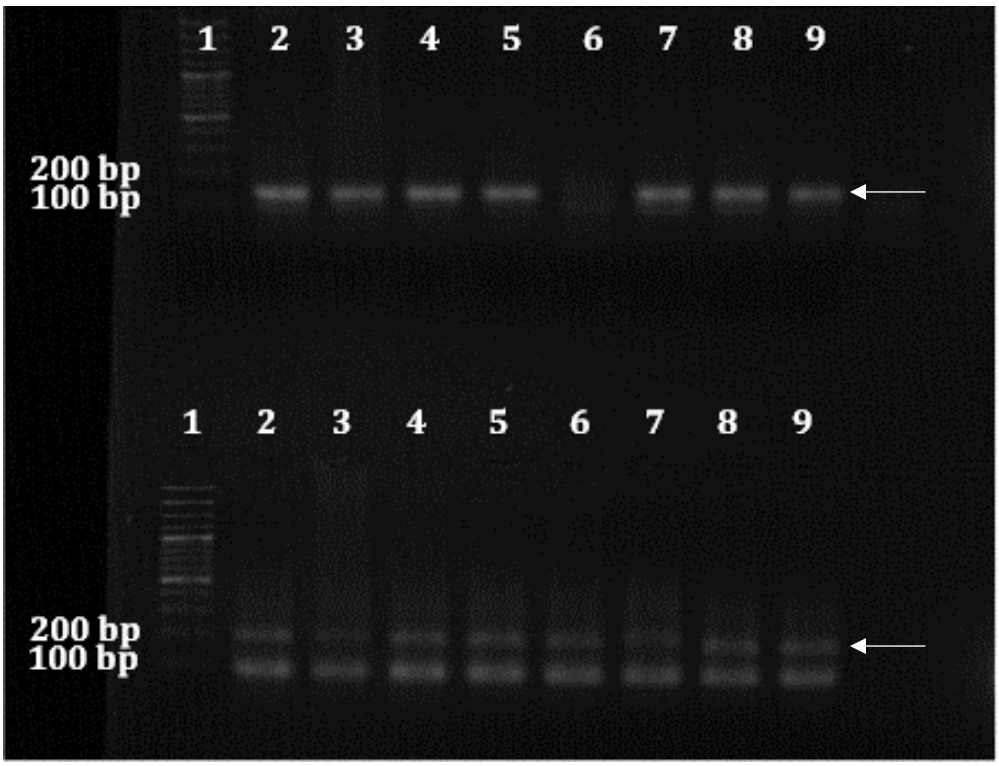

Figure 4.1.20: 2% Agarose gel showing PCR confirmation of HttQ23 and HttQ46 recombinant bacmids. (Upper 1-100 bp ladder, 2-Q23 +ve control, 3,4-Q23 S13A, 5,6,7-Q23 S13D, 8,9-Q23 S16D Lower 1-100 bp ladder, 2-Q46 +ve control, 3,4-Q46 S13A, 5,6,7-Q46 S13D, 8,9-Q46 S16D).

4.2 Expression of Huntingtin Proteins with SA or SD Mutations in *Sf9* Insect Cells and its Purification: Yields and Protein Analysis

Sf9 insect cells were revived from previously available cell stock and maintained in Sf-900 II SFM (serum-free medium). These cells were transfected with bacmids using the cationic lipid reagent Cellfectin II. Seventy-two hours post-incubation, the medium was collected to generate the P1 virus stock, and infected cells were processed for protein expression analysis by western blotting using an anti-huntingtin antibody. Expression of the huntingtin (HTT) Q23 protein was confirmed, as shown in **Fig. 4.2.1**. After verification of protein expression at the P1 stage, *Sf9* cells were infected with the P1 baculovirus stock for 72 hours to obtain the P2 virus stock. As demonstrated in **Fig. 4.2.2**, protein expression was again assessed by western blotting. Subsequently, high-titer P3 baculovirus stock was generated by infecting *Sf9* cells with the P2 stock, monitoring until ~90% cell mortality was observed, at which point HTT expression was verified. (**Fig. 4.2.3**).

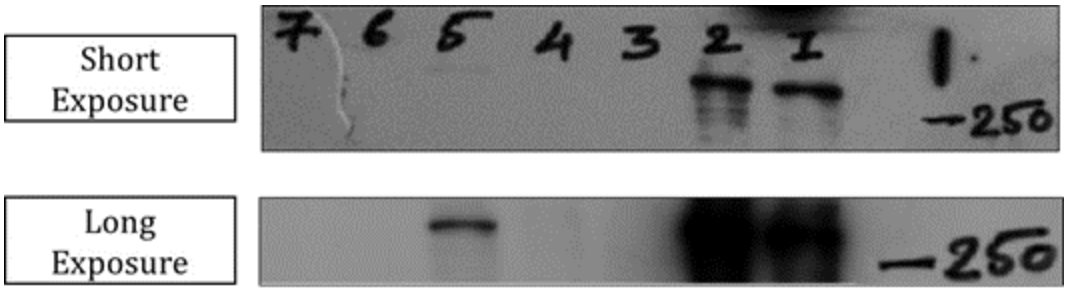

Figure 4.2.1: Western Blot image showing huntingtin expression at P1 stage (1-2 purified HTT Q23 & HTT Q32 as positive controls, 3-4 transfection controls as negative controls, 5- Q23 HTT, 6- Q46 HTT and 7- Q78 HTT).

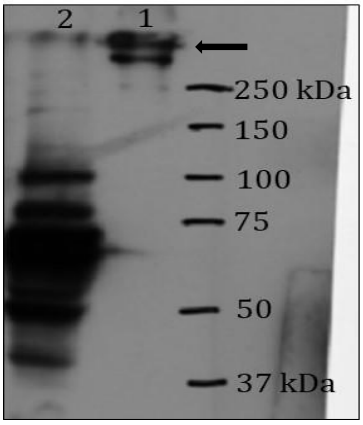

Figure: 4.2.2

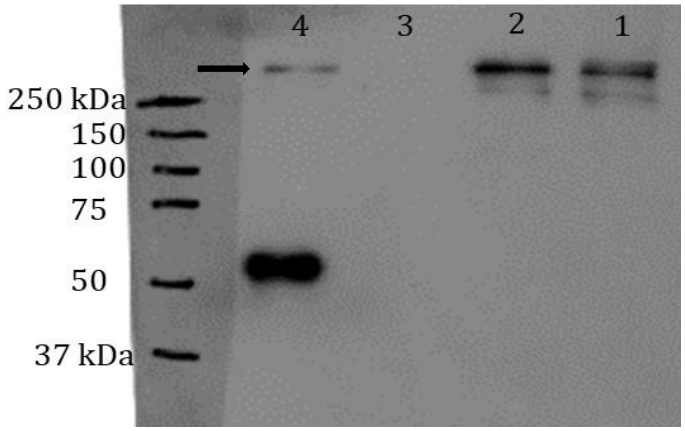

Figure: 4.2.3

Figure 4.2.2: Western Blot image showing huntingtin expression at P2 stage (1- purified Q23 as a positive control and 2- HTT Q23 huntingtin protein expressed at P2 stage).

Figure 4.2.3: Western Blot image showing huntingtin expression at P3 stage (1- HTT Q23 protein expressed at P3 stage, 2-3 HTT Q46 protein expressed at P3 stage and 4- HTT Q78 protein expressed at P3 stage).

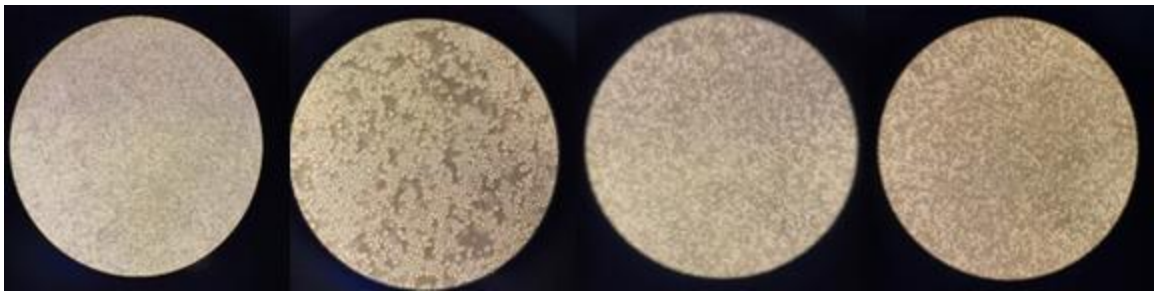

-ve Control | Infected with HTT Q23 P3 virus | Infected with HTT Q46 P3 virus | Infected with HTT Q76 P3 virus

Figure 4.2.4: Representative microscopy images showing *Sf9* cells after 72 hours post-incubation with HTT Q23, Q46 and Q78 P3 virus. Images were captured at 10X magnification.

Figure 4.2.5: Western Blot image showing huntingtin expression after 48 hours post-incubation with HTT Q23, Q46 and Q78 P3 virus.

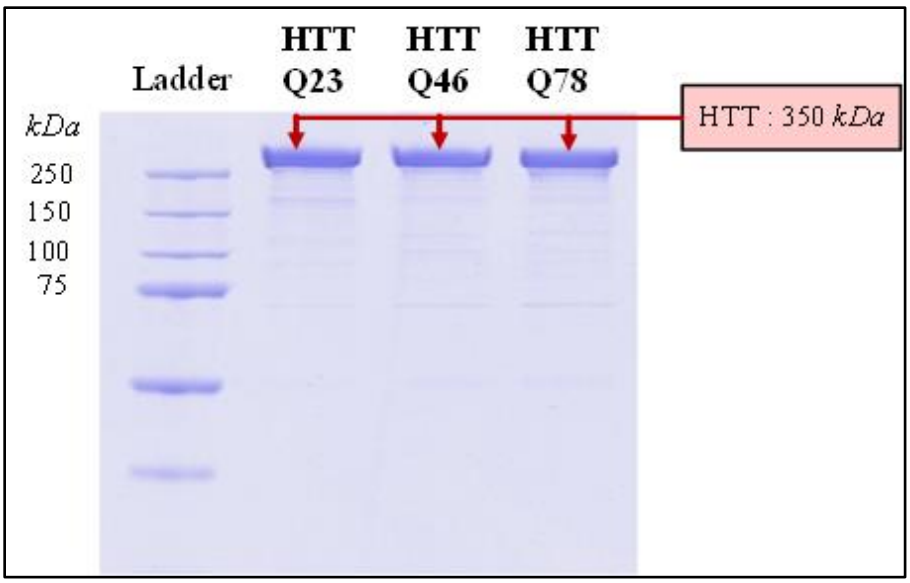

Figure 4.2.6: SDS-PAGE gel showing purified huntingtin proteins by FLAG affinity chromatography.

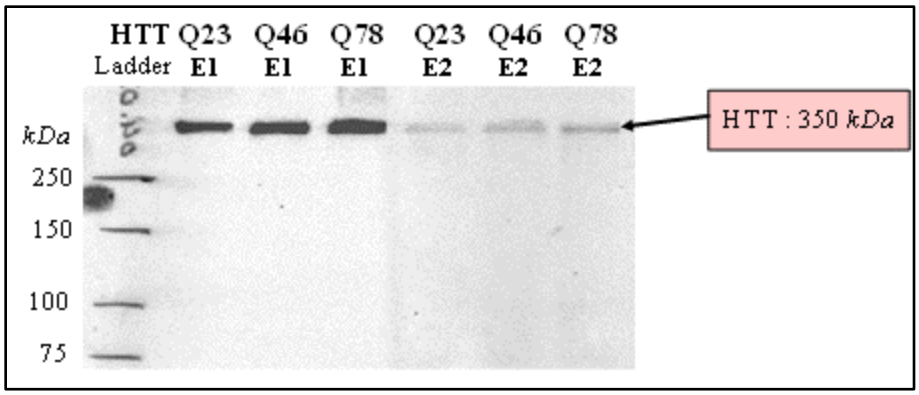

Figure 4.2.7: Western Blot image showing confirmation of huntingtin expression by FLAG affinity purification.

Healthy *Sf9* cells were infected with the HTTQ23 P3 virus stock for protein purification. After 48 hours of incubation, cells were lysed as described in the methodology section and centrifuged at 12,000 rpm for 10 minutes at 4°C. The supernatant was collected and subjected to protein purification. Wild-type HTTQ46 and HTTQ78 proteins were expressed and purified using the same procedure as for HTTQ23. Following confirmation of protein expression at the P1 stage, an equal number of *Sf9* cells were infected with the P1 baculovirus stock to obtain the P2 virus stock. *Sf9* cells were observed under an inverted microscope after 48 hours. As shown in **Fig. 4.2.4**, the swollen morphology and growth retardation of the infected cells compared to the negative control clearly indicated successful infection. High-titer P3 baculovirus stock was then generated by infecting *Sf9* cells with the P2 stock, and HTT expression was confirmed by western blotting (**Fig. 4.2.3**).

For protein purification, healthy *Sf9* cells were infected with the HTTQ46 and HTTQ78 P3 virus stocks. After 48 hours of incubation, cells were lysed and centrifuged at 12,000 rpm for 10 minutes at 4°C. The supernatant was collected and subjected to protein purification using FLAG affinity chromatography. Prior to purification, small volumes of supernatants were analyzed for HTT expression by western blotting (**Fig. 4.2.5**). The purified huntingtin protein samples were subjected to SDS-PAGE followed by Coomassie Brilliant Blue (CBB) staining to assess purity and integrity. As shown in **Fig. 4.2.6**, protein bands of approximately 350 kDa were observed. This result was

corroborated by immunoblotting, which showed band patterns identical to those seen in SDS-PAGE (**Fig. 4.2.7**).

The Recombinant huntingtin proteins with SA or SD mutations (HTTQ23 S13A/S13D/S16D and Q46 S13A/S13D/S16D) were also expressed and purified using the *Sf9* insect cell-Baculovirus system and affinity chromatography, following the same protocol. Protein bands of approximately 350 kDa were observed for these recombinant huntingtin proteins, as illustrated in **Fig. 4.2.8**. This finding was confirmed by immunoblotting, which displayed similar band patterns to those seen in SDS-PAGE (**Fig. 4.2.9**).

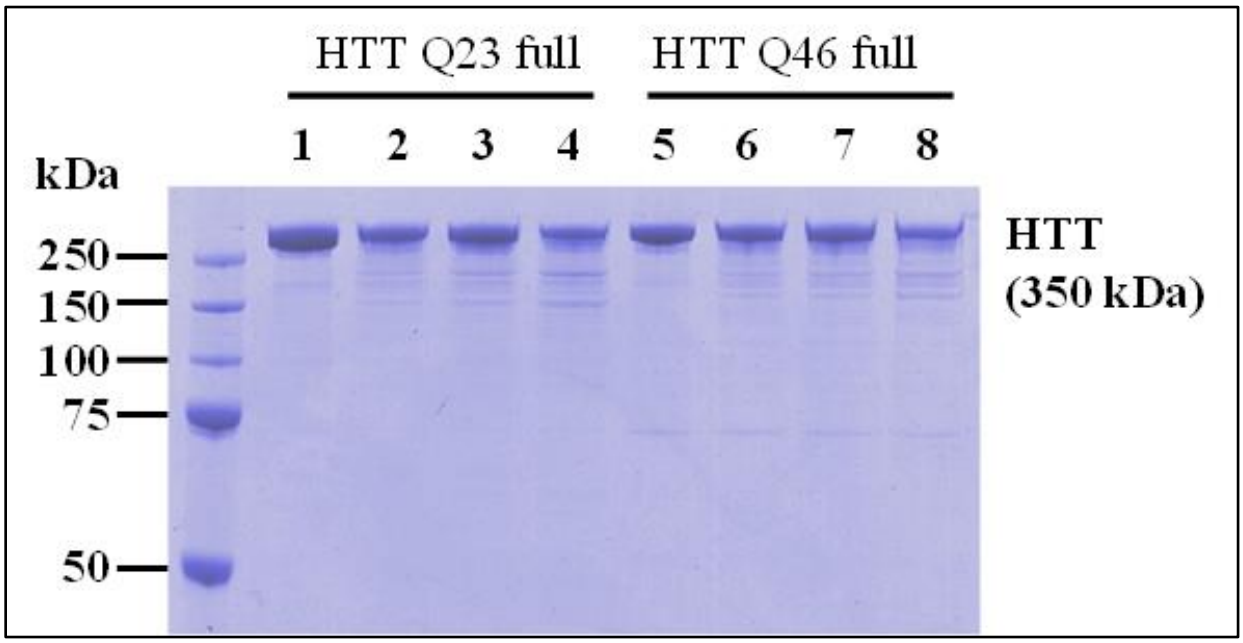

Figure 4.2.8: SDS-PAGE gel showing purified huntingtin proteins with SA or SD mutation by FLAG affinity chromatography (1. HTT Q23 wild type 2. Q23 S13A 3. Q23 S13D 4. Q23S16D 5. HTT Q46 wild type 6. Q46 S13A 7. Q46 S13D 8. Q46 S16D).

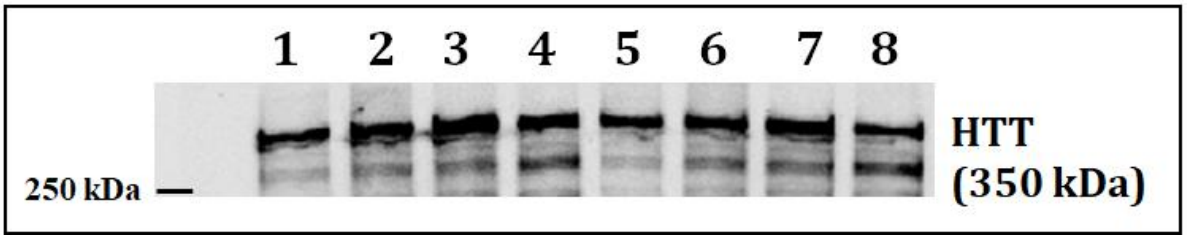

Figure 4.2.9: Western Blot image showing confirmation of recombinant huntingtin expression with SA or SD mutation by FLAG affinity purification. (1. HTT Q23 wild type 2. Q23 S13A 3. Q23 S13D 4. Q23S16D 5. HTT Q46 wild type 6. Q46 S13A 7. Q46 S13D 8. Q46 S16D).

4.3 Discussion

Phosphorylation is a critical post-translational modification that regulates protein function, stability, and localization, as well as many cellular processes [7]. This modification typically occurs at serine (S), threonine (T), or tyrosine (Y) residues, influencing protein activities, turnover, and nuclear transport [8]. In huntingtin, several phosphorylation sites have been identified, including Thr3, Ser13, Ser16, and Ser421, the latter phosphorylated by AKT [5]. The phosphorylation status of these sites has been linked to HTT's toxicity and protective roles in Huntington's disease (HD) pathology [9].

Huntingtin phosphorylation at Ser13 and Ser16 has been implicated in both neuroprotection and the modulation of HTT toxicity [6]. Phosphorylation at these sites is associated with a decrease in mutant huntingtin aggregates and an absence of HD-like phenotypes in transgenic mouse models [6]. Specifically, studies have demonstrated that while both nonphosphorylatable (SA) and phosphomimetic (SD) mutations at these sites retain essential HTT functions, only the SD mutation is linked to a significant reduction in HD pathology [6]. This suggests a protective role for Ser13/Ser16 phosphorylation against the toxic effects of mutant HTT, although the exact mechanisms remain to be elucidated.

Our study utilized site-directed mutagenesis to substitute Ser13 and Ser16 with either alanine (A) or aspartate (D), creating phosphoresistant and phosphomimetic HTT variants, respectively. These proteins served as valuable tools to investigate the functional consequences of HTT phosphorylation at these specific residues as discussed in the following chapter. The use of the *Sf9* insect cell-Baculovirus system facilitated efficient expression and purification of these HTT variants, providing high-quality protein samples for further analysis [10].

The generation of phosphomimetic and phosphoresistant mutants using such a system aligns with previously published methodologies that have successfully employed similar techniques to study protein phosphorylation and its effects on function and pathogenicity [11]. The expression and purification protocols adopted here ensure the production of sufficient quantities of HTT variants, which are crucial for detailed biochemical and functional studies.

The protective nature of Ser13/Ser16 phosphorylation in HTT highlights its potential as a therapeutic target in HD. The phosphorylation mimetics (SD) exhibited a marked reduction in HD-like symptoms and aggregates in previous studies, underscoring the therapeutic promise of

enhancing HTT phosphorylation at these sites [6]. Our findings reinforce the importance of these modifications and provide a foundation for future research aimed at deciphering the underlying mechanisms.

Future studies should focus on the detailed biochemical pathways involved in HTT phosphorylation at Ser13 and Ser16. Understanding how these modifications influence HTT interaction with other cellular proteins, its stability, and its aggregation propensity could reveal new therapeutic targets. Additionally, investigating the broader implications of HTT phosphorylation on cellular signaling pathways and neuroprotective mechanisms will be critical in developing comprehensive treatment strategies for HD.

In conclusion, the phosphorylation of HTT at Ser13 and Ser16 plays a crucial role in modulating its function and toxicity. By utilizing advanced molecular techniques, this study provides valuable tools to study role of huntingtin phosphorylation at Ser13 and Ser16 in variety of assays. Further research in this direction may pave the way for novel interventions aimed at mitigating the devastating effects of Huntington's disease.

4.4 References

1. Tözsér J, Bagossi P, Zahuczky G, Specht SI, Majerova E, Copeland TD (2003) Effect of caspase cleavage-site phosphorylation on proteolysis. The Biochemical journal 372 (Pt 1):137-143. doi:10.1042/bj20021901

2. Poon IK, Jans DA (2005) Regulation of nuclear transport: central role in development and transformation? Traffic (Copenhagen, Denmark) 6 (3):173-186. doi:10.1111/j.1600-0854.2005.00268.x

3. Aiken CT, Steffan JS, Guerrero CM, Khashwji H, Lukacsovich T, Simmons D, Purcell JM, Menhaji K, Zhu Y-Z, Green K, Laferla F, Huang L, Thompson LM, Marsh JL (2009) Phosphorylation of threonine 3: implications for Huntingtin aggregation and neurotoxicity. J Biol Chem 284 (43):29427-29436. doi:10.1074/jbc.m109.013193

4. Thompson LM, Aiken CT, Kaltenbach LS, Agrawal N, Illes K, Khoshnan A, Martinez-Vincente M, Arrasate M, O'Rourke JG, Khashwji H, Lukacsovich T, Zhu Y-Z, Lau AL, Massey A, Hayden MR, Zeitlin SO, Finkbeiner S, Green KN, LaFerla FM, Bates G, Huang L, Patterson PH, Lo DC,

Cuervo AM, Marsh JL, Steffan JS (2009) IKK phosphorylates Huntingtin and targets it for degradation by the proteasome and lysosome. J Cell Biol 187 (7):1083-1099. doi:10.1083/jcb.200909067

5. Humbert S, Bryson EA, Cordelières FP, Connors NC, Datta SR, Finkbeiner S, Greenberg ME, Saudou F (2002) The IGF-1/Akt pathway is neuroprotective in Huntington's disease and involves Huntingtin phosphorylation by Akt. Developmental cell 2 (6):831-837. doi:10.1016/s1534-5807(02)00188-0

6. Gu X, Greiner ER, Mishra R, Kodali R, Osmand A, Finkbeiner S, Steffan JS, Thompson LM, Wetzel R, Yang XW (2009) Serines 13 and 16 are critical determinants of full-length human mutant huntingtin induced disease pathogenesis in HD mice. Neuron 64 (6):828-840. doi:10.1016/j.neuron.2009.11.020

7. Cohen P (2002) The origins of protein phosphorylation. Nature Cell Biology 4 (5):E127-E130. doi:10.1038/ncb0502-e127

8. Pawson T, Scott JD (2005) Protein phosphorylation in signaling--50 years and counting. Trends in biochemical sciences 30 (6):286-290. doi:10.1016/j.tibs.2005.04.013

9. Huang WJ, Chen WW, Zhang X (2016) Huntington's disease: Molecular basis of pathology and status of current therapeutic approaches. Experimental and therapeutic medicine 12 (4):1951-1956. doi:10.3892/etm.2016.3566

10. Ross CA, Tabrizi SJ (2011) Huntington's disease: from molecular pathogenesis to clinical treatment. The Lancet Neurology 10 (1):83-98. doi:10.1016/s1474-4422(10)70245-3

11. Scherzinger E, Sittler A, Schweiger K, Heiser V, Lurz R, Hasenbank R, Bates GP, Lehrach H, Wanker EE (1999) Self-assembly of polyglutamine-containing huntingtin fragments into amyloid-like fibrils: Implications for Huntington’s disease pathology. Proceedings of the National Academy of Sciences 96 (8):4604-4609. doi:10.1073/pnas.96.8.4604